Type Ia supernovae: Advances in large scale simulation



2009 J. Phys.: Conf. Ser. 180 012023

(http://iopscience.iop.org/1742-6596/180/1/012023)

Journal of Physics: Conference Series **180** (2009) 012023 doi:10.1088/1742-6596/180/1/012023

# Type Ia Supernovae: Advances in Large Scale Simulation

**S. E. Woosley[1], A. S. Almgren[2], A. J. Aspden[2], J. B. Bell[2], D. Kasen[1], A. R. Kerstein[3], H. Ma[1], A. Nonaka[2], and M. Zingale[4]**

[1]Department of Astronomy and Astrophysics, University of California, Santa Cruz, CA 95064
[2]Center for Computational Science and Engineering, Lawrence Berkeley National Laboratory, Berkeley, CA, 94720
[3]Combustion Research Facility, Sandia National Laboratories, Livermore, CA
[4]Department of Physics and Astronomy, Stony Brook University, Stony Brook, NY, 11794-3800

E-mail: woosley@ucolick.org

**Abstract.** There are two principal scientific objectives in the study of Type Ia supernovae - first, a better understanding of these complex explosions from as near first principles as possible, and second, enabling the more accurate utilization of their emission to measure distances in cosmology. Both tasks lend themselves to large scale numerical simulation, yet take us beyond the current frontiers in astrophysics, combustion science, and radiation transport. Their study requires novel approaches and the creation of new, highly scalable codes.

## 1. Introduction

Type Ia supernovae (SN Ia) are among the brightest explosions in the modern universe and also the most regular, i.e., their brightness does not vary greatly from event to event. Those variations that do occur are correlated with other observables, such as their duration and decline rate, and this makes them very useful as "calibratable standard candles" in cosmology. The accepted paradigm that SN Ia come from the thermonuclear explosion of white dwarfs accreting mass in binary systems has been with us for almost fifty years [7], and for almost as long, scientists have tried to build realistic computer models [4]. It is a hard problem. The details of how the runaway ignites are important, yet the sparks that seed the first flames are embedded in a turbulent convective flow, and may not ignite first at the center of the star. Once ignited, the burning proceeds initially as a deflagration that is subject to several multi-dimensional instabilities which enhance the turbulence on its surface. At some density, observations strongly suggest that the flame makes a transition to detonation. A transition of this sort has no terrestrial analogue and understanding it takes us into territory unfamiliar to combustion scientists (high Karlovitz number and high Damköhler number). Finally the radiation transport is challenging. The supernova produces a glowing hot ball of radioactive ashes. The gamma-rays emitted in the decay are reprocessed into optical emission by the plasma. The debris are anisotropic and heterogeneous. It is this radiation that is ultimately observed and therefore most constraining on the models.

Our Computational Astrophysics Consortium studies all these questions and to do so is

 

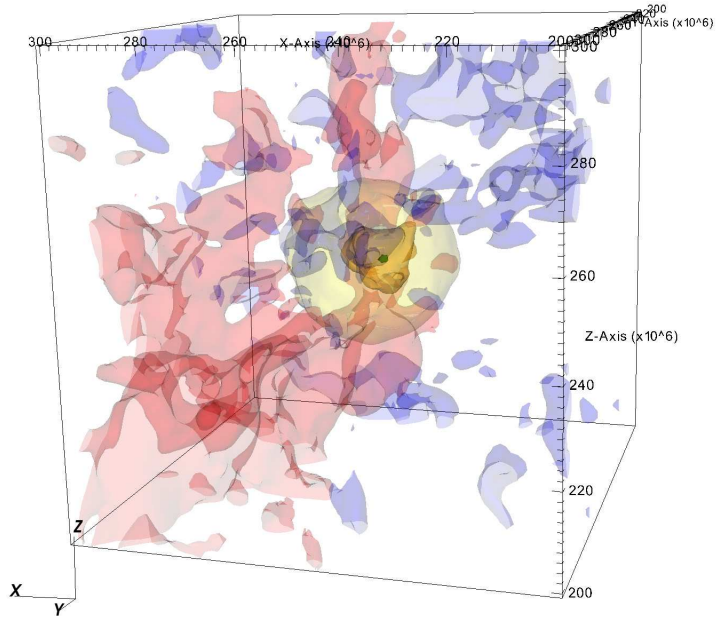


**Figure 1.** Convective motions and energy generation in a Chandrasekhar mass white dwarf at the time the first flame is born [17]. Radial velocity surfaces are colored red ($+4 \times 10^6$ cm s$^{-1}$) and blue ($-4 \times 10^6$ cm s$^{-1}$). Energy generation rate surfaces are colored yellow ($8 \times 10^{12}$ erg g$^{-1}$ s$^{-1}$) orange ($8 \times 10^{13}$ erg g$^{-1}$ s$^{-1}$), and green ($8 \times 10^{14}$ erg g$^{-1}$ s$^{-1}$). The domain shown (1000 km)$^3$ encompasses most of the convective region. Ignition occurs about 20 km from the center of mass of the star, but this is just the first ignition and other hot spots may still develop.

developing an ensemble of new scalable, multi-dimensional codes. In the following sections we briefly summarize our progress.

## 2. Ignition and the MAESTRO Code

The final explosive runaway that makes the supernova is preceded by about a century during which convection carries away an ever increasing energy generation. Finally, at some point, the time scale for further temperature increase becomes too short for convection to be efficient. It is the turbulent dynamics of this convective period that determine the initial number and location of the fusion flames that burn through the white dwarf. We have now performed the first 3D, full-star calculations of this convective phase using the new low Mach number hydrodynamics code, MAESTRO [1, 2, 3, 16, 17]. The low Mach number approximation is derived from the compressible hydrodynamics equations by decomposing the pressure into thermodynamic and dynamic components and recasting the equation of state as an elliptic constraint on the velocity field. This analytically removes acoustic waves, allowing the code to take time steps based on the advective speed rather than the sound speed.

We modeled a Chandrasekhar-mass white dwarf for its last 2 hours, watching the peak temperature rise from $6 \times 10^8$ K to over $8 \times 10^8$ K, when the first flame ignited near the center of the star. Figure 1 shows surfaces of radial velocity and nuclear energy generation rate at the point where the peak temperature crosses $8 \times 10^8$ K on its rapid rise to igniting the first flame. The reactions are strongly peaked. The radial velocity field shows a strong asymmetry—the dipole nature of this flow was first discussed in [11] and studied in [13]. Full details of this calculation are presented in [17]. The computational domain in the case shown here was $384^3$, and this one calculation required approximately 600,000 CPU-hours on the Cray XT4 machine, Jaguar, at ORNL. In the near future, we plan to run at twice the resolution in order to increase the numerical Reynolds number of the turbulent convection.

## 3. Flame Propagation in the CASTRO and SNe Codes

Once born, nuclear burning produces bubbles and sheets of hot ash embedded in cooler, denser fuel. The ash floats, producing Rayleigh-Taylor and Kelvin-Helmholtz instabilities and,

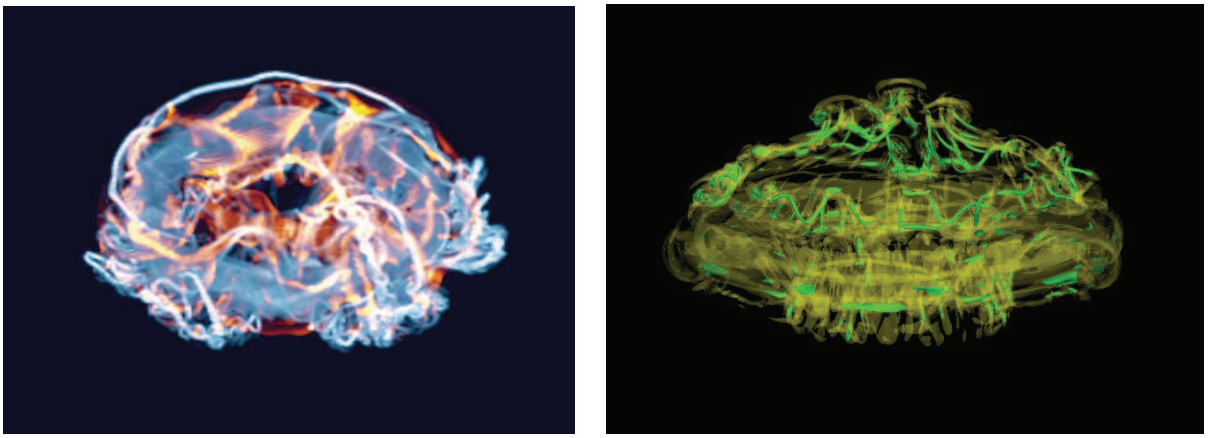

**Figure 2.** Vorticity in two floating, burning bubbles at a time when both have entered comparable non-linear phases. The bubble on the left was computed with SNe at nearly constant pressure and density. The flame was fully resolved at a density of $10^7$ g cm$^{-3}$ and the box size was 2 m. White indicates high vorticity and yellow coloration indicates regions of large nuclear energy generation. The bubble on the right was calculated with CASTRO using a thickened flame model for the burning at a density of $\sim 2 \times 10^9$ g cm$^{-3}$, gravity $1.5 \times 10^{10}$ cm s$^{-2}$, and on a scale of 100 km, comparable to the stellar scale height. The background pressure and density decreased about 50% from bottom to top. Note the tubes of high vorticity, characteristic of turbulent flow [12], in both studies. Each calculation employed a resolution of 256×256×512 zones with 2 levels of AMR and ran on 1024 CPU for about 75 hours. SNe was run on ATLAS at LLNL and CASTRO on Franklin at NERSC.

ultimately, turbulence. These instabilities, which feed back on the flame sheet, folding and distorting it, govern the rate at which the burning progresses, and, ultimately, the power and brightness of the supernova. A major effort of our Consortium has been the development of scalable codes to follow these instabilities on both large (stellar) and small (resolved flames) scales.

For small scales, we have use low-Mach number code, SNe [5, 6], developed in part with SciDAC support. This code is particularly useful for small-scale situations where the Courant condition would otherwise be prohibitive. For stellar-scale studies though, we are starting to use the new SciDAC code CASTRO. This code, developed by Almgren, Bell, and collaborators, uses compressible unsplit hydrodynamics with AMR and subcycles in time in the refined regions, resulting in considerable CPU savings. It has recently been shown to scale nearly linearly up to over 27,000 CPU at ORNL. As part of a suite of tests, we are running burning floating bubbles in planar geometry. Some results are given in Figure 2. The same generic flame and turbulence geometries appear both in calculations at low density, that well resolve the flame (SNe), and at high densities, using a thickened flame model (CASTRO). In the near future we will be moving to full star explosion models using CASTRO and a level set to track the flame.

## 4. Delayed Detonation

Detonation will not occur so long as the flame remains in the flamelet regime, regardless of how distorted the surface may become, but as the density declines, turbulence eventually tears the flame, stirring hot ash and cold fuel into a potentially explosive mixture. Using SNe, we have extended our previous study of this distributed regime [15] to larger domains. The distributed flame from Aspden *et al.* [6] was taken as a starting point. This flames was dominated by turbulent mixing so that the reactions occur at the turbulent nuclear time-scale. Damköhler [8]

| Case | (a) | (b) | (c) | (d) | (e) |
|---|---|---|---|---|---|
| Domain width ($L$) | $1.5 \times 10^2$ | $1.2 \times 10^3$ | $9.6 \times 10^3$ | $7.68 \times 10^4$ | $6.14 \times 10^5$ |
| Domain height ($H$) | $1.2 \times 10^3$ | $4.8 \times 10^3$ | $3.84 \times 10^4$ | $3.07 \times 10^5$ | $2.46 \times 10^6$ |
| Integral length scale ($l$) | $1.5 \times 10^1$ | $1.2 \times 10^2$ | $9.6 \times 10^2$ | $7.68 \times 10^3$ | $6.14 \times 10^4$ |
| Turbulent intensity ($\check{u}$) | $2.47 \times 10^5$ | $4.93 \times 10^5$ | $9.86 \times 10^5$ | $1.97 \times 10^6$ | $3.95 \times 10^6$ |
| Damköhler number ($\mathrm{Da}_T$) | $6.4 \times 10^{-3}$ | $2.6 \times 10^{-2}$ | $1 \times 10^{-1}$ | $4.1 \times 10^{-1}$ | $1.7 \times 10^0$ |

**Table 1.** Simulation properties.

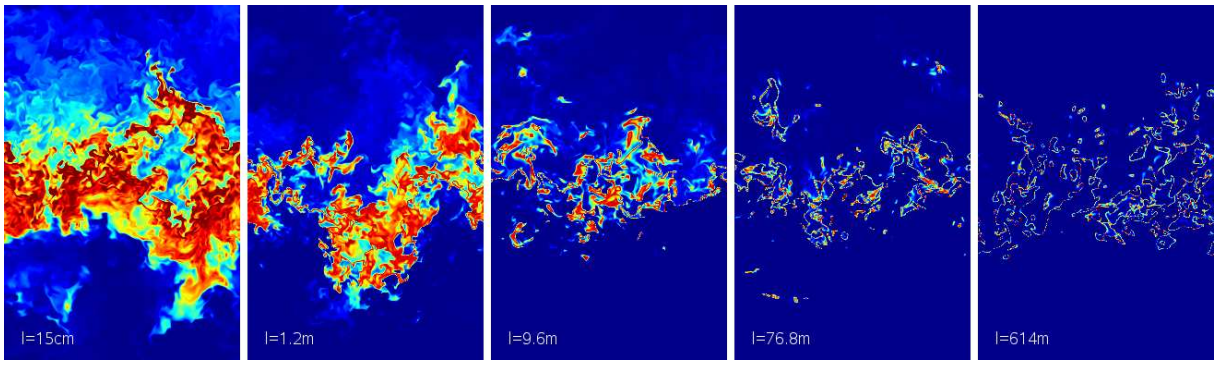


**Figure 3.** Instantaneous vertical slices of fuel consumption rate (intense burning in red, no burning in blue). The whole domain width is shown but the height is cropped. Each box is eight times as large as the previous one; the last one is 6 km across.

argued that in this "small-scale turbulence" regime ($\mathrm{Ka} \gg 1$, $\mathrm{Da} \ll 1$) mixing is dominated by a turbulent diffusion $D_T \sim \check{u}l$, where $\check{u}$ and $l$ are the turbulent intensity and integral length scale, respectively. A turbulent Damköhler number can be defined as $\mathrm{Da}_T = \tau_T/\tau^T_{\mathrm{nuc}} = l/\left(\tau^T_{\mathrm{nuc}}\check{u}\right)$, where $\tau^T_{\mathrm{nuc}} = l_T/s_T$ and $\tau_T = l/\check{u}$ are the turbulent nuclear time-scale and the turbulence time-scale, respectively, and $s_T$ and $l_T$ are the turbulent flame speed and flame width, respectively. A turbulent Karlovitz number can then be defined as $\mathrm{Ka}^2_T = \check{u}^3 l_T/s^3_T l$, so that $\mathrm{DaKa} \equiv 1$. The turbulent flame speed can be shown to scale with $s_T = \check{u}\mathrm{Da}^{1/2}_T$.

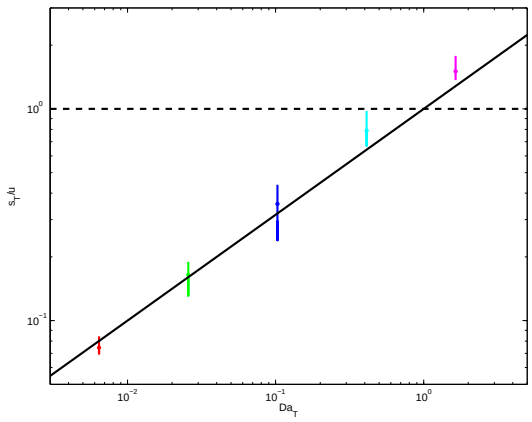


**Figure 4.** Turbulent flame speeds normalised by turbulent intensity as a function of turbulent Damköhler number. The linear scaling,$s_T = \check{u}Da^{1/2}_T$, is predicted to break down at about one.

This scaling breaks down when $\mathrm{Da}_T \approx 1$, corresponding to when the turbulent flame speed is equal to the turbulent intensity and the turbulent flame width is equal to the integral length scale. For larger length scales the turbulence can no longer affect the flame interior – the flame burns as a turbulently broadened flame with constant speed and thickness, which is moved around by the large scales. This limiting turbulent flame speed $s_\lambda$ and width $l_\lambda$ can be predicted from solely the turbulent flame speed in the original base case, $s_\lambda = \check{u}^2_0/s^0_T$ and $l_\lambda = l_u(\check{u}_0/s^0_T)^3$, where $s^0_T$, $\check{u}_0$ and $l_0$ are the turbulent flame speed, turbulent intensity and integral length scale in the base case.

Figure 3 shows slices of fuel consumption rate through the five flames. Figure 4 shows the normalised turbulent flame speed as a function of

Damköhler number. The solid black line denotes the predicted scaling $s_T = \breve{u}\mathrm{Da}_T^{1/2}$, which matches the data very well. Calculations using the Linear Eddy Model [14, 15] suggest that, for higher Damköhler numbers, the normalised flame speed levels off at a value of approximately one. The burning should also become highly irregular and potentially explosive in this regime.

An important consequence of this is that small-scale simulations can be carried out, using the three-dimensional code presented here (or using the Linear Eddy Model), to measure the turbulent flame speed under a wide range of conditions in the distributed regime ($\mathrm{Ka} \gg 1$). From these flame speeds, the limiting turbulent flame speed $s_\lambda$ can be evaluated and used as a turbulent flame model for much larger calculations in a level set code, for example.

## 5. Confronting the Observations and Cosmology

In anticipation of full star hydrodynamical models soon to be available using CASTRO, we have been improving our ability to do multi-dimensional Monte Carlo studies of radiation transport. The principal code for this purpose, SEDONA, was discussed last year [9]. More recently, we have used SEDONA to postprocess a two-dimensional survey of SN Ia explosion models calclated using the Munich SN Ia code [10]. The Munich code has the necessary physics for following both the deflagration and detonation phases of the explosion including: a) a level set approach to front tracking; b) a subgrid-model for the turbulent flame interaction; and c) the necessary nuclear physics to follow recombination and electron capture in material that is in nuclear statistical equilibrium.

The initial conditions of the explosion were selected based upon insights from our studies of ignition (Sec. 2). Specifically, from 20 to 150 ignition points were considered, distributed from the center out to $\sim 300$ km in a solid angle whose opening varied from 60° to 360°. Following the results reported last year [15] a transition to detonation was assumed when a minimal Karlovitz number and a certain range of fuel densities was achieved. Like ignition, detonation should be a stochastic process though, so five different values of Karlovitz number were considered in the range 1 to 2250 (though mostly 250 - 750).

A total of 46 hydrodynamical models was calculated and their light curves and spectra determined at all wavelengths as a function of observed angle and time. The models predict a range of $^{56}$Ni yields, from 0.3 to 1.1 solar masses. The agreement with observations shown in Figure 5 is encouraging and suggests that the models have captured the essential features of the explosion, so far as light curves and spectra are concerned. They also allow us to better understand the observed *width* of the WLR and the possible dependence of its slope on the composition of the host galaxies. In this study, the width was a consequence of the high degree of asymmetry in the explosions, caused by both asymmetric ignition and detonation. Of course we are eager to see the extent to which these results remain valid in the 3D survey we plan to carry out later this year.

## Acknowledgments

Research at LBNL was supported by the SciDAC Program under contract No. DE-AC02-05CH11231. A. Aspden was also supported by a Seaborg Fellowship. Work at UCSC was also supported by SciDAC under contract DE-FC02-06ER41438. At Sandia, research was supported by the Sandia Corporation, a Lockheed Martin Company, for the DOE under contract DE-AC04-94AL85000. M. Zingale was supported by a DOE/Office of Nuclear Physics Outstanding Junior Investigator award, grant No. DE-FG02-06ER41448, to Stony Brook. This research used resources provided by an INCITE award at the National Center for Computational Sciences at Oak Ridge National Laboratory, which is supported by the Office of Science of the DOE (DE-AC05-00OR22725), and the Franklin computer at the National Energy Research Scientific Computing Center. Additional computing resources were provided on the ATLAS Linux Cluster at LLNL as part of a Grand Challenge Project.

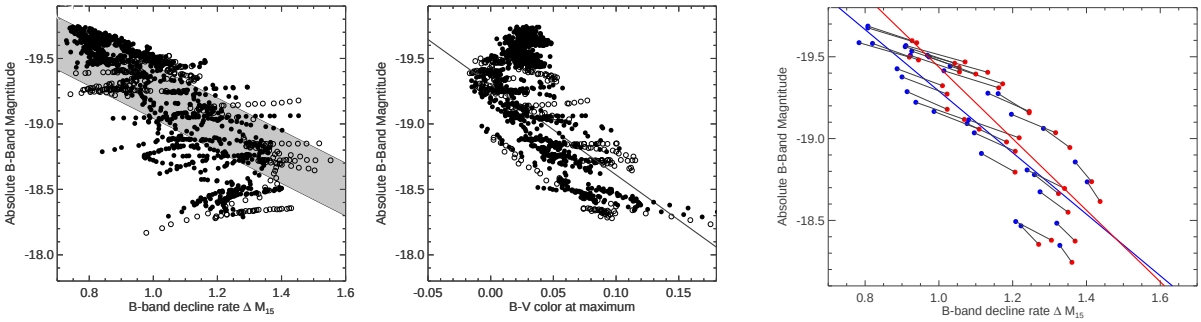


**Figure 5.** The width-luminosity relation (WLR) for SN Ia [10]. The shaded band in the left plot is the observed relation between peak brightness (absolute magnitude) and decline rate (change in B-band magnitude in 15 days after peak). Points are the result of a 2D survey of explosions described in the text. Most of the width is due to the variable angle at which an asymmetric explosion is observed. The middle plot gives the peak brightness as a function of the color of the supernova. The right hand plot shows how the angle-averaged WLR relation depends on metallicity for a range corresponding to 1/3 to 3 times solar. The different slope for the WLR for different metallicities may complicate the use of SN Ia for cosmology at the 1 - 2% level.

## References

[1] Almgren, A. S., Bell, J. B., Rendleman, C. A., & Zingale, M. 2006a, Astrophysical Journal, 637, 922
[2] —. 2006b, Astrophysical Journal, 649, 927
[3] Almgren, A. S., Bell, J. B., Nonaka, A., & Zingale, M. 2008, Astrophysical Journal, 684, 449
[4] Arnett, W. D. 1969, Astrophysics and Space Science, 5, 180
[5] Bell, J. B., Day, M. S., Rendleman, C. A., Woosley, S. E., & Zingale, M. A. 2004, J. Comput. Phys., 195, 677
[6] Aspden A. J., Bell J. B., Day M. S., Woosley S. E. & Zingale M. 2008 Astrophysical Journal, 689, 1173
[7] Hoyle, F., & Fowler, W. A. 1960, Astrophysical Journal, 132, 565
[8] Damköhler G. 1940 *Z. Elektrochem* 46, 601 – 652
[9] Kasen, D., Thomas, R. C., Röpke, F., & Woosley, S. E. 2008, Journal of Physics Conference Series, 125, 012007
[10] Kasen, D., Röpke, F., & Woosley, S. E. 2009, submitted to Nature.
[11] Kuhlen, M., Woosley, S. E., & Glatzmaier, G. A. 2006, Astrophysical Journal, 640, 407
[12] Sreenivasan, K. R., & Antonia, R. A. 1997, Annual Review of Fluid Mechanics, 29, 435
[13] Woosley, S. E., Bell, J. B., Glatzmaier, G., Kasen, D., Nugent, P., Röpke, F., & Zingale, M. 2007, Journal of Physics Conference Series, 78, 012081
[14] Woosley, S. E., Kerstein, A., Sankaran, V., and Röpke, F. 2009, Astrophysical Journal, submitted, astroph-0811-3610.
[15] Woosley, S. E., Aspden, A. J., Bell, J. B., Kerstein, A. R., & Sankaran, V. 2008, Journal of Physics Conference Series, 125, 012012
[16] Zingale, M., Almgren, A. S., Bell, J. B., Malone, C. M., Nonaka, A. 2008, Journal of Physics Conference Series, 125, 012013
[17] Zingale, M., Almgren, A. S., Bell, J. B., Nonaka, A., & Woosley, S. E. 2009, ApJ, submitted.